J. Math. Biol. (1998) 36: 249–268

Journal of Mathematical Biology

Kinetic model of *Proteus mirabilis* swarm colony development

Sergei E. Esipov[1], **J. A. Shapiro**[2,*]

[1] James Franck Institute and the Department of Physics, University of Chicago, 5640 S. Ellis avenue, Chicago, IL 60637, USA
[2] Department of Biochemistry and Molecular Biology, Cummings Life Sciences Center, 920 E. 58th street, Chicago, IL 60637-4931, USA

Received 3 July 1996; received in revised form 9 December 1996

Abstract. *Proteus mirabilis* colonies display striking symmetry and periodicity. Based on experimental observations of cellular differentiation and group motility, a kinetic model has been developed to describe the swarmer cell differentiation-dedifferentiation cycle and the spatial evolution of swimmer and swarmer cells during *Proteus mirabilis* swarm colony development. A key element of the model is the age dependence of swarmer cell behaviour, in particular specifying a minimal age for motility and maximum age for septation and dedifferentiation to swimmer cells. Density thresholds for collective motility by mature swarmer cells serve to synchronize the movements of distinct swarmer cell groups and thus help provide temporal coherence to colony expansion cycles. Numerical computations show that the model fits experimental data by generating a complete swarming plus consolidation cycle period that is robust to changes in parameters which affect other aspects of swarmer cell migration and colony development. The kinetic equations underlying this model provide a different mathematical basis for a temporal oscillator from reaction-diffusion partial differential equations. The modelling shows that *Proteus* colony geometries arise as a consequence of macroscopic rules governing collective motility. Thus, in this case, pattern formation results from the operation of an adaptive bacterial system for spreading on solid substrates, not as an independent biological function. Kinetic models similar to this one may be applicable to periodic phenomena displayed by other biological systems with differentiated components of defined lifetimes.

Key words: Aging models – Kinetic equation – Cooperative processes – Collective behavior – Cellular differentiation

* Corresponding author: Phone 773-702-1625, Fax 773-702-0439, Email: jsha@midway.uchicago.edu

I Statement of the biological problem

Bacterial colonies are excellent experimental material for studying the behavior and evolution of complex self-organizing systems (Shapiro, 1995). The colonies of *Proteus mirabilis* are especially interesting because their morphogenesis involves periodic oscillation between phases of migration over the substrate (swarming) and phases of growth within stationary populations (consolidation) (Belas, 1997). *Proteus* colonies present two key problems: (1) to account for their deceptively simple circular symmetry and regular terracing (Fig. 1) and (2) to explain the robust periodicity of cyclic behavior under conditions when the velocity and duration of swarming are variable (Rauprich et al., 1996). We believe that the two problems are related and will argue below that they have a common solution in density-dependent collective motility. With regard to colony periodicity, we particularly wished to investigate whether the observed robust clock-like behavior could be explained without invoking dedicated oscillators to control the initiation of each swarming cycle.

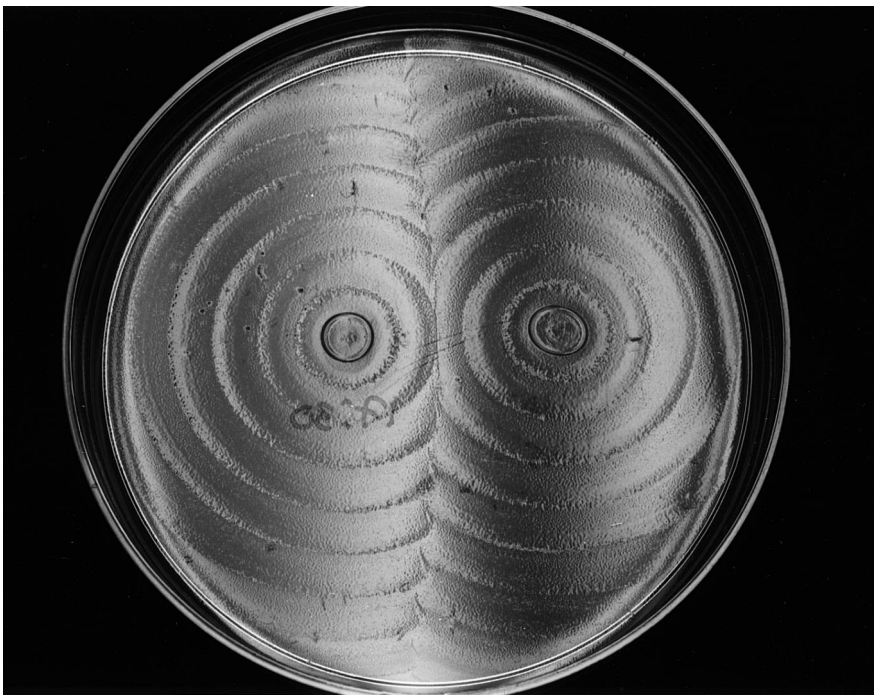

Fig. 1. Two *Proteus mirabilis* colonies after less than two days' incubation at 32 °C on our standard laboratory medium containing 2% agar (Rauprich et al., 1996). The PRM1 colony on the right was 43 hours old, and the PRM1 colony on the left was 40 hours old. Note that the phase difference between the two colonies was maintained and that there was no entrainment of the swarm terraces

II Formulation of the mathematical model

The most dramatic feature of *Proteus* colony development is the involvement of specially differentiated cells in the migratory phase (Hauser, 1885; Russ-Münzer, 1935; Kvittingen, 1949). In liquid medium, *Proteus* cultures consist virtually exclusively of short oligoflagellated "swimmer" cells comparable in their behavior to motile *E. coli*. Swimmer cells go through a prototypical bacterial cell growth and division cycle. On agar medium, however, a second channel of cellular behavior appears: some cells cease septation but continue to grow and produce many lateral flagella to form elongated multi-nucleoid hyperflagellated "swarmer" cells which aggregate in parallel arrays to form motile multicellular "rafts" (Klieneberger-Nobel, 1947; Hoeniger, 1964, 1965, 1966; Jones and Park, 1967; Williams and Schwarzhoff, 1978). Only swarmer cells in contact with other cells are capable of translocation over surfaces of medium containing $\geqq 1\%$ agar; swimmer cells and isolated swarmer cells are immobile (Sturdza, 1973b). Thus, swarm motility is an inherently cooperative process resulting in nonlinear transport of the population characterized by expansion dependent on bacterial density. After some time migrating, swarmer cells have been observed to cease movement, septate and produce groups of swimmer cells which can then undergo the typical cell division cycle (Klieneberger-Nobel, 1947; Hoeniger, 1964). Thus, in the expanding *Proteus* colony, there are two connected patterns of cellular development (Fig. 2). In addition to these microscopic observations, macroscopic results on the lag time needed to initiate swarming and the effect of agar concentration on colony expansion point to density-dependent thresholds in the initiation of each swarming phase (Moltke, 1929; Rauprich et al., 1996).

A Basic parameters of the model

We make use of three phenomena based on experiment – (i) interlocking cell cycles, (ii) collective motility and (iii) density-dependent thresholds – to account for the periodic behavior of *Proteus* colonies. The local kinetics of population structure involve the following ingredients:

* Each swarmer cell is assigned an age, θ, so that the continuous description contains a distribution function, $\rho_s(\boldsymbol{r}, \theta, t)$ for the number of swarmers of a given age θ at the point $(\boldsymbol{r}, t)$, where $\boldsymbol{r}$ is the two-dimensional vector characterizing each point in space at time t. For the present, we ignore the age distribution of swimmers.

* $0 \leqq \xi \leqq 1$ describes the differentiation factor which is the fraction of swimmers per division that enter the swarmer development channel with an initial age $\theta = 0$. Treating ξ as a constant would be an obvious oversimplification because we know that swarmer cell differentiation is regulated, at least by medium factors and the presence or absence of a high viscosity environment (Dick et al., 1985; Belas, 1997). Based on the observation that the inner colony zones are occupied only by swimmers (Russ-Münzer, 1935),

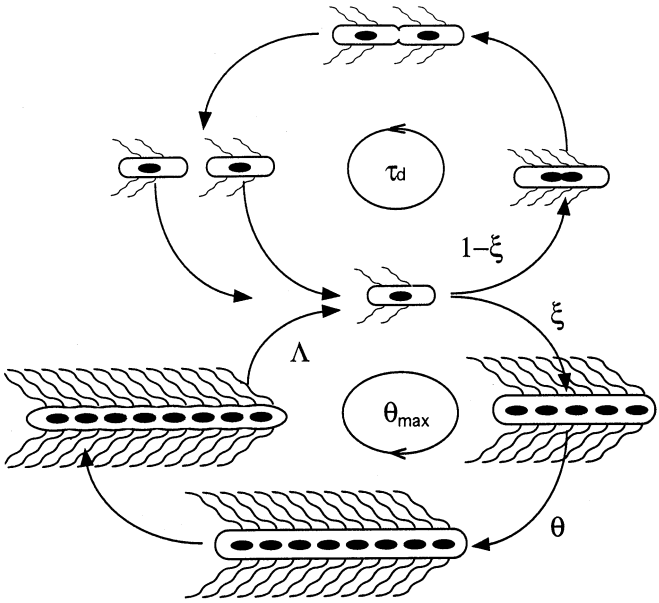

Fig. 2. Schematic representation of the two interlocking cell cycles of *Proteus mirabilis*. The top cycle illustrates the cell growth and division process of swimmers, which cannot migrate over solid surfaces. The bottom cycle illustrates the differentiation, aging and dedifferentiation of elongated, hyperflagellated swarmers which can assemble in rafts and migrate collectively over agar medium. The parameters (Model A) are explained in the text

we assume that $\xi = 0$ at concentration of swimmers above a certain value (see below).

* As swarmer development proceeds, $\theta_{\min}$ denotes the age when the swarmer cell can participate actively in group migration, i.e. acquires a "driver's license". We do not yet have experimental data on swarmer life spans, but the appearance of large numbers of short swimmers as each new terrace undergoes consolidation suggests that the typical lifespan is on the order of the swarming + consolidation cycle (Russ-Münzer, 1935; Kvittingen, 1949). We have modeled swarmer lifespan in two ways. Model A assumes that swarmers have a fixed maximal age, $\theta_{\max}$, and they septate deterministically upon reaching this age. Model B assumes that there is a constant probability of septating per unit time, $1/\theta_{\max}$, so that $\theta_{\max}$ is only an average lifespan.

* $\Lambda(\theta)$ is the rate at which swarmer cells of age θ septate. In Model A the septation rate is defined only for maximal age, $\Lambda(\theta) = \delta(\theta - \theta_{\max})$, in Model B the septation rate does not depend on age at all, $\Lambda(\theta) = \theta_{\max}^{-1}$.

* Swarmers have the same DNA/length ratio as swimmers (Klieneberger-Nobel, 1947; Hoeniger, 1966), and we assume that biomass increase during

swarmer development occurs at the same rate as during the swimmer cell cycle. Thus, a swarmer of age θ will be $\exp(\theta/\tau_d)$ larger than its parent swimmer, where τ_d is the characteristic growth time. The number of swarmers produced in a septation event from a single swarmer is given uniquely by $\exp(\theta_{\max}/\tau_d)$ in Model A and varies as $\exp(\theta/\tau_d)$ in Model B.

$*$ Surface densities of swimmer and swarmer cell populations will be indicated by the capital letters P_c and P_s, respectively (c for consolidation phase, s for swarming phase). While we do not resolve swimmers in age, the surface density of swarmers is related to a biomass weighted average over the ages, with e^{θ/τ_d} being the contribution of age θ.

As mentioned above, the process of swarmer cell differentiation doesn't occur at concentration of swimmers where $P_c \geqq P_{c,\mathrm{sat}}$ (saturation).

B Description of local kinetics

The equations for local kinetics of *Proteus* population structure are:

$$\frac{\partial P_c(t)}{\partial t} = \frac{(1-\xi)P_c(t)}{\tau_d} + \int_0^t \mathrm{d}\theta \rho_s(\theta, t)\Lambda(\theta)e^{\theta/\tau_d} \tag{1a}$$

$$\frac{\partial \rho_s(\theta, t)}{\partial t} + \frac{\partial \rho_s(\theta, t)}{\partial \theta} = \frac{\xi P_c}{\tau_d}\delta(\theta) - \rho_s(\theta, t)\Lambda(\theta)\ . \tag{1b}$$

There is no term for nutrient depletion in these equations, and no equation for nutrient changes. We have chosen to make these omissions because we are primarily interested in movement of the colony front, and experimental results indicate that exponential biomass increase continues in the colony interior for at least two swarming + consolidation cycles (Rauprich et al., 1996). Thus, all the pertinent dynamics occur in a regime of saturating nutrient, and the consequences of nutrient depletion are felt only at later stages of colony morphogenesis, which we do not consider here.

Different terms describe the local kinetics of specific processes. The left-hand side (LHS) of Eq. (1a) represents the change in time of the swimmer population based on exponential increase of the non-differentiating fraction $(1-\xi)$ and the characteristic growth parameter τ_d (first, right-hand-side (RHS) term) plus the septation of swarmers distributed in age (hence, integral) into swimmers with the rate $\Lambda(\theta)$, where each septation event produces e^{θ/τ_d} swimmers (second RHS term). These relationships keep biomass unchanged by the alternative cell cycle. The change in time of the swarmers of a given age, θ, is expressed by the first term in the LHS of Eq. (1b). This change is the combined result of the swarmer aging process (second term on the LHS), differentiation of the fraction ξ of the swimmer population to produce swarmers of age $\theta = 0$ (symbolized by the delta-function $\delta(\theta)$ in the first term on the RHS), and loss of swarmers due to septation with rate $\Lambda(\theta)$ (second term on the RHS). Note that the swarmer aging process enters into these equations in two places: as the integral on the RHS of Eq. (1a) and as the

second differential term on the LHS of Eq. (1b). These two terms distinguish Eqs. (1) from partial differential equations (PDEs), as in reaction-diffusion formulations (Levin and Segel, 1985; Murray, 1993).

The analytical solution of the system (1) for Model A may be written as a recursion valid at times $n\theta_{\max} \leqq t \leqq (n+1)\theta_{\max}$, where n is a nonnegative integer:

$$P_c(t) = P_c(n\theta_{\max}) e^{\frac{(1-\xi)(t-n\theta_{\max})}{\tau_d}} + \frac{\xi}{\tau_d} e^{\frac{(1-\xi)t+\theta_{\max}}{\tau_d}} \int_{n\theta_{\max}}^{t} dt' P_c(t'-\theta_{\max}) e^{-\frac{(1-\xi)t'}{\tau_d}}, \quad (2a)$$

$$\rho_s(\theta, t) = \frac{\xi}{\tau_d} P_c(t-\theta), \quad (2b)$$

$$P_s(t) = P_c(0) e^{\frac{t}{\tau_d}} - P_c(t), \quad (2c)$$

and the initial condition $P_c(0)$ must be supplied. Applying the recursion rule many times, a series in powers of t and exponentials is obtained. The solution of model B may be obtained by a Laplace transform,

$$P_c(t) = \frac{P_c(0)}{1 + \frac{\tau_d}{\xi\theta_{\max}}} \left\{ \frac{\tau_d}{\xi\theta_{\max}} \exp\left(\frac{t}{\tau_d}\right) + \exp\left[\frac{t(\theta_{\max}(1-\xi)-\tau_d)}{\theta_{\max}\tau_d}\right] \right\} \quad (3a)$$

$$\rho_s(\theta, t) = \frac{\xi}{\tau_d} P_c(t-\theta) \exp\left(-\frac{\theta}{\theta_{\max}}\right) \quad (3b)$$

with Eq. (2c) indicating $P_s(t)$.

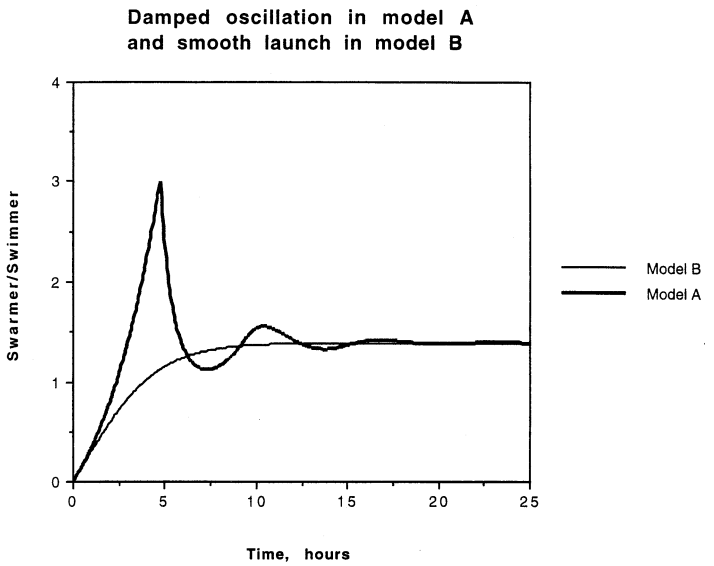

Fig. 3. The local kinetics of the swarmer/swimmer biomass ratio P_s/P_c over time according to Eqs. (2) and (3). The heavy line gives the numerical results for Model A, and the thin line for Model B

Models A and B display very different temporal dynamics when local growth begins with a pure swimmer population (Fig. 3). Model A produces damped oscillations of the swarmer/swimmer ratio, while Model B produces a smooth curve without oscillations. Observations on the kinetics of swarmer production by an exceptional *Proteus* isolate which differentiates in liquid medium agree with the predictions of Model A (Dick et al., 1985).

C Description of spatially resolved kinetics

After *Proteus* swimmers are inoculated on agar medium, there is a lag phase before colony expansion begins, and the length of this delay depends inversely upon the concentration of the inoculum down to a minimum value characteristic for each set of conditions (Rauprich et al., 1996). This observation suggests that a certain threshold concentration of swarmers has to accumulate before motion begins. Density-dependence of *Proteus* mobility is also inherent in the collective nature of swarmer cell movement in rafts (Sturdza, 1973b). We denote the initial motility threshold as $P_{s,\max}$ and assume that diffusivity of the population is initially zero at smaller values of the concentration of motile swarmers, $P_s = \int_{\theta_{\min}}^{\theta_1} d\theta \rho_s(\boldsymbol{r}, \theta, t)$, $\theta_1 = \theta_{\max}$ in Model A, $\theta_1 = t$ in Model B. When swarming begins, however, the rafts spread over the substrate, and their average concentration diminishes, but motility continues for a particular length of time depending upon conditions (Rauprich et al., 1996). To describe this particular kind of nonlinear behavior, we formulate a designated local memory field, called motility status or m. If $P_s \geqq P_{s,\max}$, then $m = 1$ and remains at that value until $P_s \leqq P_{s,\min}$, when $m = 0$. It should be noted that the memory field, m, is a property of the local swarmer population at each position, not of individual cells, because it depends on P_s. We assume the reason that motility switches off once per swarming phase and does not restart until after the following consolidation phase is that new swarmers are only produced from swimmers. Swarmers age but do not divide until they reach the septation stage, at which point they septate into swimmers rather than into younger swarmers. Consequently, the leading cohort of swarmers in each swarm phase is constrained to undergo a decrease in P_s and move upwards in age distribution towards septation as it moves outwards from the previous terrace. The aging process will accelerate the decrease in P_s as mature swarmers are lost through dedifferentiation. Since older dense population of swimmers ($P_c \geqq P_{c,\mathrm{sat}}$) do not produce swarmers (see above), only the new swimmer population created by septation events can effectively generate a new swarmer population with density exceeding $P_{s,\max}$ to initiate the next swarming phase. The first terrace represents an exception which we do not consider in detail here.

The existence of $P_{s,\min}$ is justified by the experimental observation that motility ceases when the expanding population still contains swarmer cells that can be reactivated to migrate in the subsequent swarm phase (Bisset and Douglas, 1976). We model the macroscopic motion of the population by

nonlinear diffusion known to be capable of producing moving fronts (Landau and Lifshitz, 1987; Murray, 1993). The swarmers' diffusivity is assumed to be

$$D(P_c, P_s, m) = D_0 m(\boldsymbol{r}, t)\, f\left(\frac{P_s}{P_{s,\max}}\right) \exp\left(-\frac{P_c}{P_{c,\mathrm{sat}}}\right), \tag{4a}$$

$$f = (x - x_{\min})\Theta(x - x_{\min})\,. \tag{4b}$$

In these equations D_0 is the amplitude of diffusivity, $x = P_s/P_{s,\max}$, $x_{\min} = P_{s,\min}/P_{s,\max}$, $\Theta(x)$ is the step-function: $\Theta(x) = 1$ at $x \geqq 0$, and $\Theta(x) = 0$ otherwise. The exponential decay of diffusivity at high concentrations of immobile cells describes the inability of swarmers to invade zones containing high concentrations of swimmers, $P_c > P_{c,\mathrm{sat}}$; (unpublished videotapes). Other expressions for diffusivity dependence on swarmer concentration, $f = x$, $f = x^2, f = 1$, all gave qualitatively similar results to the formulation in (4b) in our numerical computations. Since $f(x)$ acts in conjunction with thresholds, even the case of $f = 1$ gives highly nonlinear results.

Diffusion of swarmers can be added to the right-hand-side of Eq (1b) to give spatially resolved kinetics, and the full system of kinetic equations becomes

$$\frac{\partial P_c}{\partial t} = \frac{[1 - \xi(P_c)]\, P_c}{\tau_d} + \int_0^t \mathrm{d}\theta \rho_s \Lambda \mathrm{e}^{\theta/\tau_d} \tag{5a}$$

$$\frac{\partial \rho_s}{\partial t} + \frac{\partial \rho_s}{\partial \theta} = \frac{\xi(P_c) P_c}{\tau_d}\, \delta(\theta) - \rho_s \Lambda + \nabla \cdot [D(P_c, P_s, m)\, \nabla \rho_s]\,, \tag{5b}$$

Eqs. (5) indicate that transport of swarmers is cooperative: the rate is determined by the integral concentration of all different swarmers, and motile swarmers of all ages move with the raft velocity. The solution of Eqs. (5) with linear diffusion does not generate continuous oscillations for either model.

III Results of numerical computations based on the model

We have performed numerical integration of Eqs. (5) in one spatial dimension by a simple difference method. Local kinetics was updated by a first order Euler scheme, and the time step Δt was maintained not larger than about $\tau_d/100$. We implemented linear transport along a discretized θ axis by shifting over one lattice site $\Delta\theta$ each $\Delta\theta/\Delta t$ time steps. This updating is free from numerical diffusion along the θ axis. The first site ($\theta = 0$) was filled at each time step by differentiation of swimmers. Nonlinear diffusion in real space was performed by determining the motility status, m, at each mesh point in space, transferring the prescribed amount of swarmers from each motile point individually to neighboring points, and receiving the corresponding amount from those points for which $m = 1$. The finite difference scheme for Eqs. (5) was simply

$$\frac{P_{c_{n+1,m}} - P_{c_{n,m}}}{\Delta t} = \frac{[1 - \xi(P_{c_{n,m}})]\, P_{c_{n,m}}}{\tau_d} + \sum_0^{k_{\max}} \Delta\theta \rho_{s_{n,m,k}} \Lambda \mathrm{e}^{\theta_k/\tau_d} \tag{6a}$$

$$\frac{\rho_{s_{n+1,m,k}} - \rho_{s_{n,m,k}}}{\Delta t} = (\rho_{s_{n,m,k-1}} - \rho_{s_{n,m,k-1}})\delta_{n,n_\theta} \tag{6b}$$

$$+ \frac{\xi(P_{c_{n,m}})P_{c_{n,m}}}{\tau_d}\delta_{k,0} - \rho_{s_{n,m,k}}\Lambda_k + \frac{J_{n,m+1/2,k} - J_{n,m-1/2,k}}{(\Delta x)^2} \tag{6c}$$

$$J_{n,m,k} = D_{n,m+1/2} \quad \rho_{s_{n,m+1/2,k}} - D_{n,m-1/2} \quad \rho_{s_{n,m-1/2,k}} . \tag{6d}$$

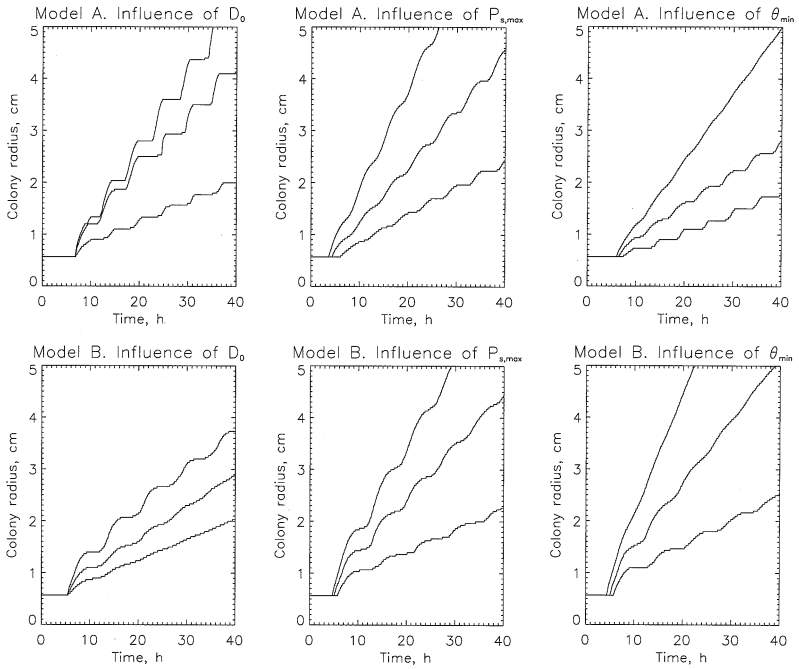

Fig. 4. Predicted increase of the colony radius over time at different values of D_0, $P_{s,\max}$, and $\theta_{\min}$ according to Model A (top panels) or Model B (bottom panels). The fixed parameters in these computations (unless explicitly specified below) were: $\xi = 0.5$ (we expect $\xi \sim O(1)$ from the lag phase measurements (Rauprich et al., 1996)); $t^* = 15$ h (after this time has passed upon bacteria arrival at a given location, local nutrient supply is assumed to be exhausted, and growth is accomplished, cf. Rauprich et al., 1996); $\tau_d = 1.7$h (computed from the lag phase measurements, Rauprich et al., 1996); $\theta_{\max} = 4.7$ h (Model A, to focus on differences between τ_p and $\theta_{\min}$), and $\theta_{\max} = 2.0$ h (Model B, to generate realistic values of τ_p); $\theta_{\min} = 0.35\theta_{\max}$ (to ensure periodicity in both models); $P_{c,\text{sat}} = \exp(4.7/1.7) = 15.8744$ a.u. (in arbitrary units); $P_{s,\max} = 10$ a.u. (Model A), $P_{s,\max} = 2.0$ a.u. (Model B); $P_{s,\min} = P_{s,\max}/2$ (O(1) denominator); $D_0 = 0.01$ cm^2/sec (Model A, to generate realistic expansion rates), $D_0 = 0.03$ cm^2/sec (Model B). The variable parameters were the following (from the top to bottom curves). Influence of D_0: (Model A) $D_0 = (0.045, 0.036, 0.015)$ cm^2/sec; (Model B) $D_0 = (0.008, 0.020, 0.035)$ cm^2/sec. Influence of $P_{s,\max}$: (Model A) $P_{s,\max} = (0.126, 0.252, 0.567)P_{c,\text{sat}}$; (Model B) $P_{s,\max} = (0.063, 0.094, 0.157)P_{c,\text{sat}}$. Influence of $\theta_{\min}$: (Model A) $\theta_{\min} = (0.15, 0.30, 0.55)\theta_{\max}$, $D_0 = 0.02$ cm^2/sec; (Model B) $\theta_{\min} = (0.15, 0.25, 0.35)\theta_{\max}$. The source codes can be found via anonymous ftp at debye.uchicago.edu. Login name: ftp, password: esipov@franck.uchicago.edu, directory: /pub

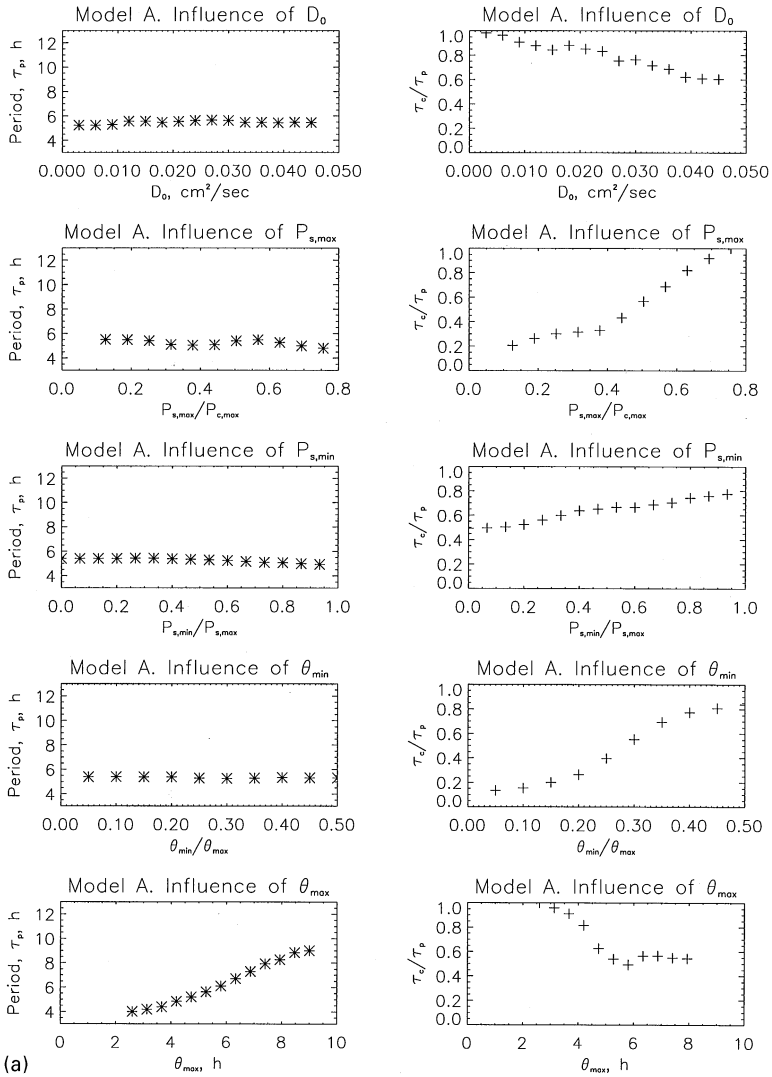

Fig. 5a and b. Effect of varying different parameters on the length of τ_p, the cycle period (asterisks), and on C, the consolidation phase as a fraction of the complete cycle (crosses). **a** Model A. **b** Model B. Plots from the top row for each model: (first row) influence of the amplitude of diffusivity, D_0 in cm^2/sec; (second row) influence of the upper swarming threshold, $P_{s,\max}$, in units of the maximum swimmer concentration for swarmer differentiation, $P_{c,\mathrm{sat}}$; (third row) influence of the lower swarming threshold, $P_{s,\min}$, in units of $P_{s,\max}$; (fourth row) influence of the "driver's license" age, $\theta_{\min}$, in units of $\theta_{\max}$; (fifth row) influence of the maximal swarmer age, $\theta_{\max}$, in hours. The basic set of parameter values used in the computations is given in the legend to Fig. 4. In several computations, values in this

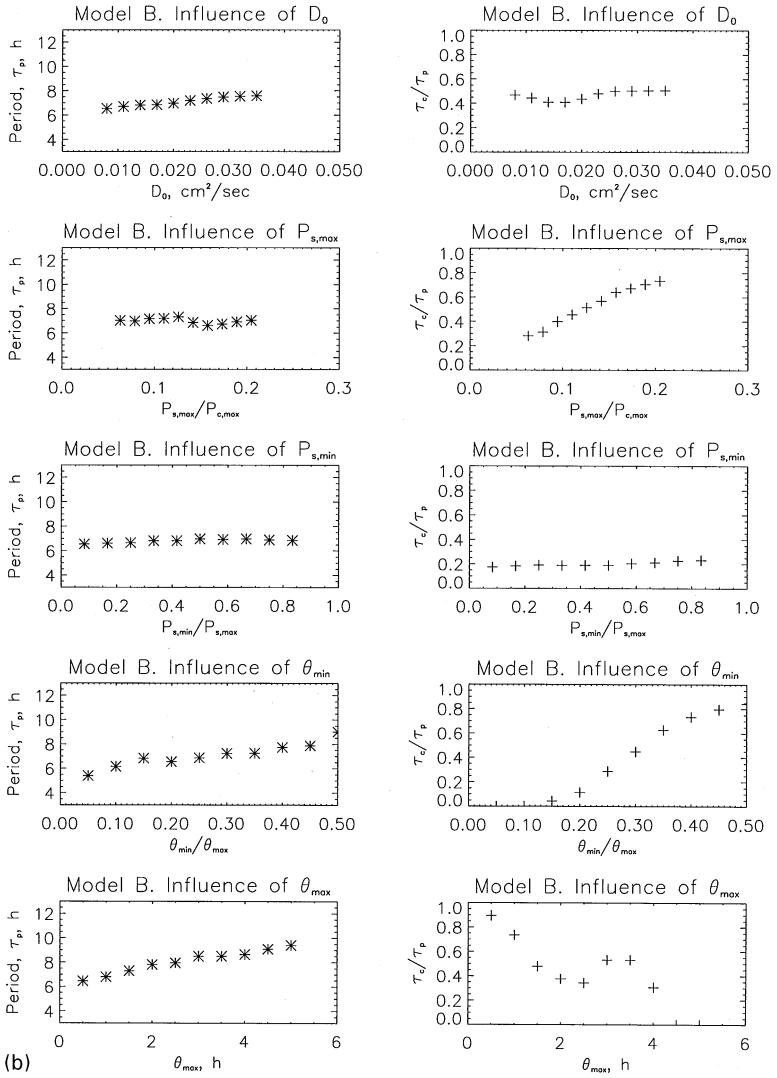

set were changed in order to fit the results into a numerical "Petri dish" of 10 cm diameter: (Model A) (third row) $D_0 = 0.03$ cm^2/sec, (fourth and fifth row) $D_0 = 0.02$ cm^2/sec; (Model B) (third row) $P_{s,\max} = 0.063 P_{c,\mathrm{sat}}$. Numerical values of τ_p were obtained by smoothing the step-like results of computations (see Fig. 4) and accumulating the time intervals between the ($\pm$) inflection points for each curve. To measure the consolidation time the histogram of displacements during each period was obtained, and the time interval corresponding to a 10% contribution to the histogram was computed. This procedure gives positive values for any discrete periodic curve, but is sufficient to observe the trends

Diffusivity is computed according to Eqs. (4) with local values of the fields involved. The motility status is a local function of the swarmer density as described above. Here index n refers to discretization in time, m – in space, k – in age, so that $k_{\max}$ refers to the maximal age group, $n_\theta = \Delta\theta/\Delta t$. Auxiliary discrete field $J_{n,m,k}$ is the diffusive flux. Where the code generated smooth fields, we did not exhaustively investigate the range of discretization parameters. The results were obtained with lattices containing $\geqq 300$ spatial mesh points and 20 age groups (although we tested up to 70 age groups). It took about 10 minutes on a Silicon Graphics workstation to do a well resolved simulation.

Figure 4 shows the envelope kinetics produced by the two models at several values of D_0, $P_{s,\max}$, and $\theta_{\min}$. While both models produce periodic motion, only Model A gives oscillations of fixed amplitude similar to experimental results throughout the parameter space we have explored so far. When the dependence of cycle period, τ_p, on parameters D_0, $P_{s,\max}$, $P_{s,\min}$, $\theta_{\min}$, and $\theta_{\max}$ was measured for Model A, we found the expected monotonic dependence on $\theta_{\max}$ but an unexpected robustness to changes in the other four parameters ($\leqq 10\%$ variation in τ_p). In contrast, the fraction of the total cycle occupied by the consolidation phase was sensitive to variations in all five parameters (Fig. 5). This behavior is similar to the observed response of *Proteus* colonies to changes in agar concentration (Rauprich et al., 1996). We know from observation that changing agar concentration alters the rate of expansion (Rauprich et al., 1996), and it is logical to assume that agar concentration also affects the cellular and group requirements for motility represented by $P_{s,\max}$, $P_{s,\min}$, $\theta_{\min}$. For example, Sturdza has observed that larger rafts form at the start of swarming on higher agar concentrations (Sturdza, 1973a). By choosing appropriate values for two (D_0, $P_{s,\max}$) out of five parameters (D_0, $P_{s,\max}$, $P_{s,\min}$, $\theta_{\min}$, and $\theta_{\max}$) we have produced acceptable fits to experimental data (Fig. 6).

In contrast to Model A, Model B generates periodic behavior only in certain parameter ranges. Oscillations of fixed amplitude occur when D_0 and $\theta_{\min}$ are high, strengthening the synchronizing effect on nonlinear transport (see Sect. IVA below). Oscillations are damped for lower values of $\theta_{\min}$ and D_0. In Model B, period dependencies are more pronounced and may indicate some transitions (Fig. 5).

On the basis of our numerical computations, we believe that Model A more closely reproduces experimental results and that a fixed swarmer cell lifespan, $\theta_{\max}$, is more likely to be applicable to the cellular differentiation cycle in actual *Proteus* colonies.

While it is tempting to assume that robust periodicity in Model A is a trivial consequence of a fixed $\theta_{\max}$, it is important to note that $\tau_p > \theta_{\max}$, and that the two do not show a simple linear relationship (Fig. 5). One could further suppose that the cycle period reflects the time needed for newly dedifferentiated swimmer cells to re-enter the swarming age dimension, which is of the order of τ_d/ξ, but our computations also indicate that $\tau_p \leqq \theta_{\max} + \tau_d/\xi$. Thus, the observer, τ_p values for Model A differ from both

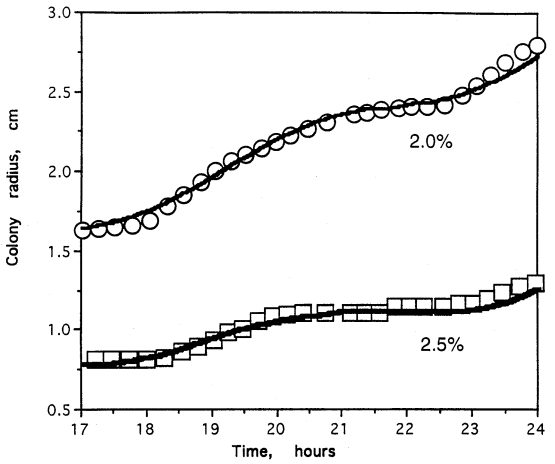

Fig. 6. Numerical fits (Model A) to experimental data for the dependencies of colony radius on time at 2.0% and 2.5% agar concentration (Rauprich et al., 1996). For 2.0% agar, $D_0 = 0.08$ cm^2/sec, $P_{s,\max} = 0.47\, P_{c,\mathrm{sat}}$; for 2.5% agar, $D_0 = 0.05$ cm^2/sec, $P_{s,\max} = 0.57\, P_{c,\mathrm{sat}}$. The other parameters were at the values given in the legend to Fig. 4

trivial expectations and imply a more interesting dynamic based on Eqs. (5) which produce interlocking oscillations in mobile and immobile cell populations. These dynamics can be observed in sequential snapshots of the spatially resolved age distribution (Fig. 7). At the end of swarming and the start of the consolidation phase (t_1), there is a bimodal swarmer distribution consisting of older cells near $\theta_{\max}$ and younger cells near $\theta = 0$. As the consolidation phase continues (t_2), many of the older swarmers reach $\theta_{\max}$ and septate, while the younger swarmers mature and are joined by the newly differentiated cells. When the swarmer population achieves $P_{s,\max}$ and the next swarming phase begins (t_3), the swarmer population is unimodal and biased towards $\theta_{\min}$. As swarming proceeds (t_4), the swarmer population ages and the peak moves closer to $\theta_{\max}$, so that some of the swarmers begin to septate. This alternation in the structure of the swarm and consolidation populations corresponds to the situation described by Bisset and Douglas in *Proteus* colonies; they found that some active swarmer cells cease movement at the end of each swarm phase, do not dedifferentiate, and recover motility at the start of the subsequent swarm phase (Bisset and Douglas, 1976). We have confirmed this by our own videotape observations.

IV Discussion

A Sources of periodic behavior

Our minimal goal in elaborating a mathematical model was to find out whether an independent clocklike controller was necessary to explain our

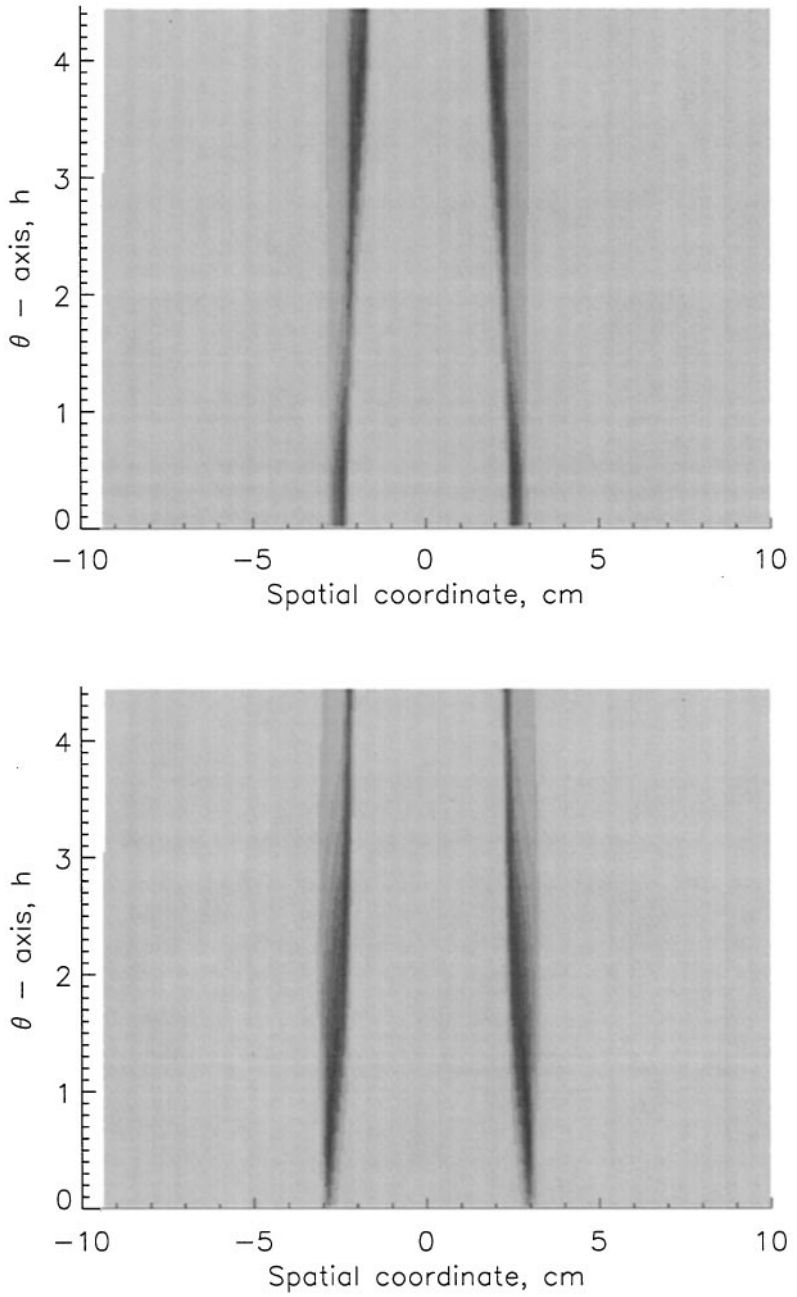

Fig. 7. Snapshots of the numerically obtained age distribution of the swarmer population, $\rho(x, \theta, t)$ at four successive time points $t_1 = 20.8h$, $t_2 = 22.4h$, $t_3 = 23.6h$, $t_4 = 24.8h$ in the Proteus cycle. The magnitudes of ρ are shown as inverse gray scale representations (the larger is ρ the darker is the corresponding point on the snapshot) in an age-space, (θ, x), plot

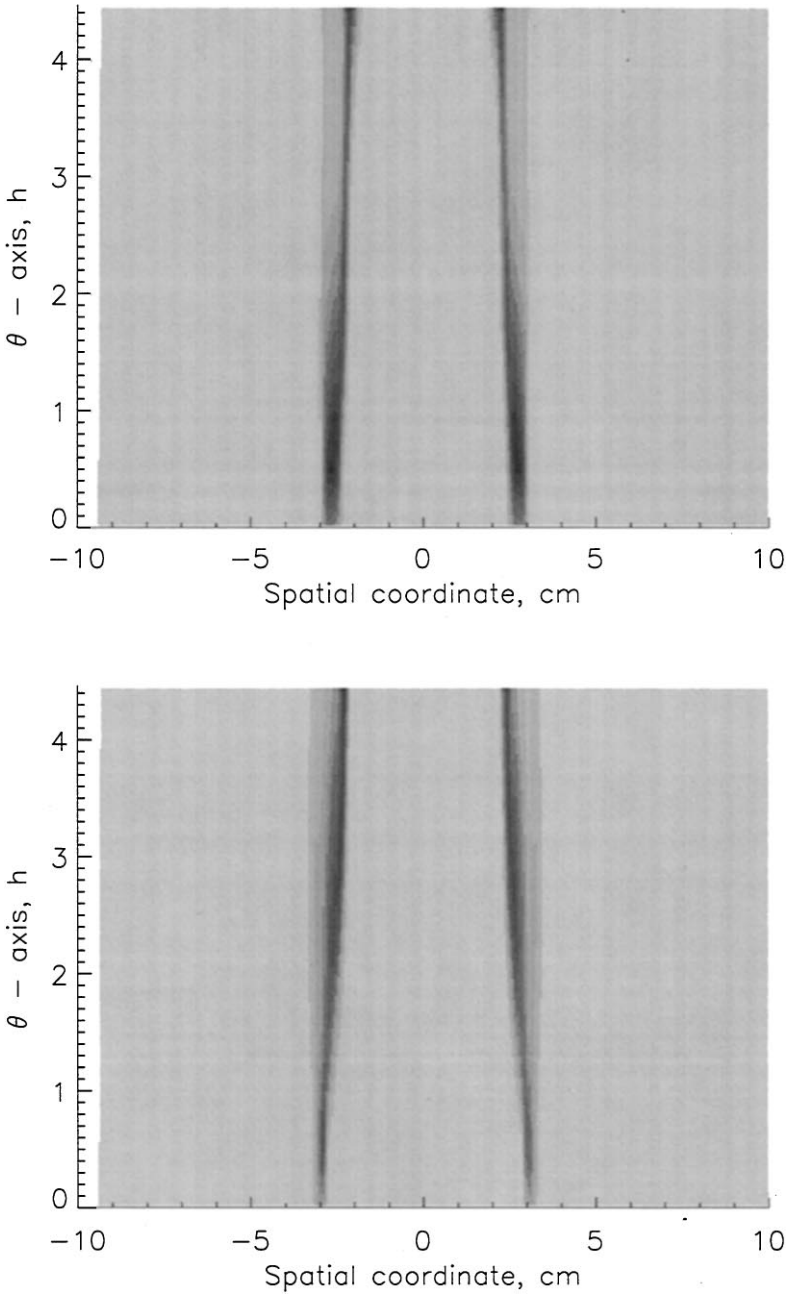

at the start of the consolidation phase (t_1, upper left), the middle of the consolidation phase (t_2, upper right), the start of the swarm phase (t_3, lower left), and the middle of the swarm phase (t_4, lower right). The basic parameters used are given in the Fig. 4 caption (Model A). One parameter was modified: $P_{c,\mathrm{sat}} = 20$ (a.u.)

observation that the duration of the swarming + consolidation cycle in *Proteus* colonies is robust to many treatments which alter the velocity and duration of the swarming phase (Rauprich et al., 1996). The results of computations presented in Figs. 4, 5 and 6 show that we can obtain such robust periodic behavior with a model based on the known phenomena of bacterial differentiation and multicellular interactions without invoking an extra oscillating system. In other words, at a given temperature and range of agar concentrations, the *Proteus* swarm colony is itself a clock.

There are two principle sources for robust periodicity in Model A. The first source is a fixed lifetime, $\theta_{\max}$, for the differentiation-dedifferentiation cycle (Fig. 1). The importance of a fixed $\theta_{\max}$ is apparent from comparing the results of computations based on Models A and B (Fig. 5). In Model A $\theta_{\max}$ sets a lower bound for the cycle period, τ_p. The second source of robust periodicity in both models is the density-dependent nonlinear diffusivity represented in our model by the motility field, m, and the swarming thresholds $P_{s,\max}$ and $P_{s,\min}$. Nonlinear diffusivity is a consequence of the collective nature of *Proteus* swarm migration, which involves both the organization of swarmer cells into multicellular rafts (Sturdza, 1973a; Williams and Schwarzhoff, 1978) and extracellular polysaccharides shared by the cells within rafts and larger swarm populations (Stahl et al., 1983; Gygi et al., 1996).

The role of nonlinear diffusivity is to synchronize populations which would otherwise begin to lose coherence as they accumulate small deviations in the timing of individual swarmer groups. This synchronizing effect can be understood intuitively by considering what happens at the end of a particular consolidation phase. If a local subpopulation near the colony perimeter achieves $P_{s,\max}$ before its neighbors, its swarmers will begin to migrate outwards and enter zones where P_s is lower and the swarmers are still immobile. As long as the neighboring subpopulations are below $P_{s,\min}$, the premature motion will eventually cease, and such local "false starts" will die out. But when the neighboring subpopulations approach $P_{s,\min}$, the swarmers spreading from local centers will stimulate the additional subpopulations to join the migration. These false starts will tend to equalize local differences in P_s, and entire regions will achieve $P_{s,\max}$ and become motile in a more or less synchronized fashion. In fact, the kind of behavior just described has been observed in time-lapse videotapes of the second and subsequent swarm phases in *Proteus* colonies: shortly before broad swarm groups emerge from the colony perimeter, rhythmic surface displacements are seen to start locally, increase in intensity and spread circumferentially around the colony about 0.1 mm inside the edge (Shapiro and Trubach, 1991; unpublished videotapes).

Although we have not yet been able to carry out numerical computations in two and three dimensions, we anticipate that the thresholds governing non-linear diffusivity will have a parallel smoothing effect on the colony circumference. If this inference proves correct, then the remarkable concentric symmetry and periodicity of *Proteus mirabilis* colonies on laboratory media result from the process of collective motility utilizing specialized cells of defined lifetime, not from a dedicated morphogenetic program.

B Comparison with reaction-diffusion systems and possible mathematical novelty

In approaching the task of modelling the periodic behavior of *Proteus* colonies, we initially expected to apply a series of partial differential equations (PDEs) of the kind used in reaction-diffusion models (Levin and Segel, 1985; Murray, 1993). In the reaction-diffusion models, different fields prescribe a rate of change for the concentration of particular reactants at each point in space and time, and the future evolution of the system is a function exclusively of the instantaneous distribution of reactants. Reaction-diffusion PDEs offered no obvious way to incorporate the age distribution characterizing the swarmer cell differentiation-dedifferentiation cycle. There is no way to reduce the description from our kinetic equations to reaction-diffusion PDEs because the future evolution of the density fields is a function both of the present distribution of microscopic elements (cells) as well as the past sequence of events (their ages).

We call our model a kinetic model because it is based on a Boltzmann-like kinetic equation (Boltzmann, 1923) in which there is evolution along an age (θ) axis in addition to evolution along space and time axes. Certain properties of the system are represented by integrals over θ, such as diffusivity [Eq. (4a)]. Our model resembles, in some respects, previous work on spatial diffusion of age-dependent populations (Gurtin, 1973). Kubo and Langlais (1991) treated periodic spatial structures, but their analysis used linear diffusion and assumed an external periodic source for new members of the population. In their analysis of periodic spatial patterns in sea shells, Ermentrout et al. (1986) invoked difference equations based on pre-existing finite time increments. Busenberg and Ianelli (1983) and Kim (1996) studied non-linear diffusion in age-dependent populations but did not address periodic behavior. Thus, to our knowledge, this is the first attempt to describe periodic non-linear population expansion based solely on the internal dynamics of age structure.

C Biological applicability

The kinetic model is based on parameters deduced from the known phenomena of *Proteus* swarm colony development. While there are many possible alternative formulations for these parameters, we have not had to introduce any purely *ad hoc* elements into the equations. The cellular differentiation-dedifferentiation cycle and collective motility have been observed directly, and density-dependent thresholds and nonlinear diffusivity are strongly indicated by observations on the timing of swarming (Rauprich et al., 1996).

The model predicts that migration initiates as the consequence of population dynamics rather than as a response to the depletion of nutrients (Moltke, 1929) or the accumulation of negative chemotactic factors (Lominski and Lendrum, 1947). Thus, according to the model, the observed dependence of colony periodicity on temperature and nutritional factors (Rauprich et al.,

1996) would be explicable as a secondary result of altering cellular growth dynamics. There is experimental evidence in favor of the idea that swarmer cell aggregation is sufficient to initiate swarming and that the duration of the swarming and consolidation phases is independent of direct nutritional control. Sturdza observe that swarmer cells could initiate migration within minutes after transplantation to fresh agar medium which was not depleted and contained no negative chemotactic substances (Sturdza, 1973a, c), and he demonstrated that the initiation of motility by transplanted swarmers was density-dependent (Sturdza, 1973b). We found that initial carbon source concentration (hence the time needed for nutrient depletion) did not affect the timing of the swarming plus consolidation cycle and that swarming initiated many hours before exponential growth ceased in the colony interior (Rauprich et al., 1996). Finally, the absence of entrainment between out-of-phase colonies (Fig. 1) indicates that timing of the swarming and consolidation phases does not result from response to an external field of diffusible signals but is internal to each developing colony.

The fact that the kinetic model generates periodic behavior and can produce numerical computation results which fit experimental observations is encouraging. However, the ultimate test of the model lies in exploring its predictions. A bimodal distribution of swarmer cell ages at consolidation plus quantitative agreement of the observer $\theta_{\max}$ and cycle period values with the relationships in Fig. 5 will be strong evidence in favor of the kinetic model. Natural strains of *Proteus* differ in their colony morphologies, lag times and cycle periods (Rauprich et al., 1996; unpublished observations). It is also possible to obtain *Proteus* mutants which have altered colony morphogenesis patterns (Allison and Hughes, 1991; Belas et al., 1991). Applying the kinetic model, it should be possible to predict which genetically-controlled aspects of cellular behavior are able to account for the distinct colony phenotypes. Thus, tests of the model's validity can be conducted by measuring the values for parameters such as ξ and $\theta_{\max}$ for different *Proteus* strains. In order to study swarmer cell age distributions, new methods will need to be developed. These will involve observations of cell length profiles using microscopes and flow cytometers. It should also be possible to follow the fate of individual swarmer cells by fluorescent labelling in non-fluorescent populations (cf. Siegert and Weijer, 1992; Sager and Kaiser, 1994). In conjunction with these experimental investigations, it will be important to explore the statistical basis in cell populations of our continuous averaged macroscopic description.

Bacterial colonies, even of populations derived from a single cell, are organized structures composed of multiple cell types (Shapiro, 1988, 1995). They are the simplest experimentally accessible ecosystems. Principles which apply to colonies may well prove valid for more complex ecologies. It is not hard to envisage multispecies ecosystems in which functionally specialized components arise with distributed lifespans. If these components are involved in expansion, then there would be an ecosystem essentially similar to the *Proteus* colony which could display similar kinds of periodic behaviors. Since the kinetic equations can generate oscillations (Figs. 3 and 4) and are distinct

from reaction-diffusion PDEs, they may provide new mathematical models for spatio-temporal oscillators. Thus, we would not be surprised to learn that formulations similar to these kinetic equations will find applications to systems other than *Proteus* colonies.

Acknowledgements. We are grateful for fruitful conversations with T. Dupont, B. Ayati, H. Riecke, M. Matsushita and O. Rauprich. N. Koppel, A. Winfree, L. Segel, D. Tieffry, and T. Dupont helped us by their illuminating critical remarks regarding the manuscript. This work was supported in part by the MRSEC Program of the National Science Foundation under the Grant Number DMR-9400379 administered through the University of Chicago.

References

Allison, C. and Hughes, C.: Closely linked genetic loci required for swarm cell differentiation and multicellular migration by *Proteus mirabilis*, Mol. Microbiol. **5**, 1975–1982 (1991)

Belas, R., Erskine, D. and Flaherty, D.: *Proteus mirabilis* mutants defective in swarmer cell differentiation and multicellular behavior. J. Bacteriol. **173**, 6279–6288 (1991)

Belas, R.: *Proteus mirabilis* and other swarming bacteria, in J. Shapiro and M. Dworkin (eds.) Bacteria as Multicellular Organisms (pp. 183–219), Oxford University Press, NY (1997)

Bisset, K. A. and C. W. I. Douglas.: A continuous study of morphological change in the swarm of *Proteus*. J. Med. Microbiol. **9**, 229–231 (1976)

Boltzmann, L. Vorlesungen über Gastheorie, ed. J. A. Barth, Leipzig (1923)

Busenberg, S. and Ianelli, M.: A class of nonlinear diffusion problems in age-dependent population dynamics, Nonlinear Anal., Theory Methods Appl. **7**, 501–529 (1982)

Dick, H., Murray, G. E. and Walmsley, S.: Swarmer cell differentiation of *Proteus mirabilis* in fluid media. Canadian J. Microbiol., **31**, 1041–1050 (1985)

Ermentrout, B., Campbell, J. and Oster, G.: A Model for Shell Patterns Based on Neural Activity, The Veliger **28**, 369–388 (1986)

Gurtin, M. E.: A system of equations for age-dependent population diffusion, J. Theor. Biol. **40**, 389–392 (1973)

Gygi, D., Rahman, M. M., Lai, H.-C., Carlson, R., Guard-Petter, J. and Hughes, C.: A cell surface polysaccharide that facilitates rapid population migration by differentiated swarm cells of *Proteus mirabilis*. Molec. Microbiol. **17**, 1167–1175 (1996)

Hauser, G.: Uber Faulnissbacterien and deren Beziehungen zur septicamie., F.G.V. Vögel, Leipzig, p. 18 (1885)

Hoeniger, J. F. M.: Cellular changes accompanying the swarming of *Proteus mirabilis*. I. Observations on living cultures, Canadian J. Microbiol., **10**, 1–9 (1964).

Hoeniger, J. F. M.: Development of flagella by *Proteus mirabilis*, J. Gen. Microbiol., **40**, 29–42 (1965)

Hoeniger, J. F. M.: Cellular changes accompanying the swarming of *Proteus mirabilis*. I. Observations of stained organisms, Canadian J. Microbiol., **12**, 113–122 (1966)

Jones, H. E. and Park, R. W. A.: The short forms and long forms of *Proteus*, J. Gen. Microbiol. **47**, 359–367 (1967)

Kim, M.-Y.: Galerkin methods for a model of population dynamics with nonlinear diffusion, Num. Methods for Part. Diff. Eqs., **12**, 59–73 (1996)

Klienberger-Nobel, E.: Morphological appearances of various stages in *B. Proteus* and *Coli*. J. Hyg. **45**, 410–412 (1947)

Kvittinger, J.: Studies of the life-cycle of *Proteus hauser*. Part 3. Acta Pathol. Microbiol. Scand., **32**, 24–50; ,855–878 (1949)

Kubo, M. and Langlais, M.: Periodic solutions for a population dynamics problem with age-dependence and spatial structure. J. Math. Biol. **29**, 363–378 (1991)

Landau, L. D. and Lifshitz, E. M.: Fluid Mechanics, pp. 344–345, 2nd ed., Pergamon Press, NY (1987)
Levin, S. A. and Segel, L. A.: Pattern Generation in Space and Aspect. SIAM Review, **27**, 45–67 (1985).
Lominski, I. and Lendrum, A. C.: The Mechanism of Swarming of *Proteus*. J. Path. Bact. **59**, 688–691 (1947)
Moltke, O.: Untersuchungen über das Phänomen des Schwärmens der Proteus-Bazillen. Centralbl. f. Bakt. etc. I. Abt. Originale, **11**, 399–403 (1929)
Murray, J. D.: Mathematical Biology, 2nd ed. Springer Verlag, NY (1993)
Rauprich, O., Matsushita, M., Weijer, K., Siegert, F., Esipov, S. E. and Shapiro, J. A. Periodic phenomena in *Proteus mirabilis* swarm colony development, J. Bacteriology, **178**, 6525–6538 (1996).
Russ-Münzer, A.: Das Schwärmphänomen bei *Bacillus proteus*. Zentralb. Bakteriol. Parasitenkd. Infectionskr. Hyg. Abt. I. Orig. **133**, 315–318 (1935)
Sager, B. and Kaiser, D.: Intercellular C-signaling and the traveling waves of *Myxococcus*. Genes & Development. **8**(2), 2793–2804 (1994)
Shapiro, J. A. and Trubach, D.: Sequential events in bacterial colony morphogenesis, Physica D, **49**, 214–223 (1991)
Shapiro, J. A.: Bacteria as multicellular organisms, Scientific American, **256**(6), 82–89 (1988)
Shapiro, J. A.: The significance of bacterial colony patterns, BioEssays, **17**, 597–607 8(1995)
Siegert, F. and Weijer, C. J.: Three-dimensional scroll waves organize *Dictyostelium* slugs. Proceedings of the National Academy of Sciences of the United States of America. **89**(14), 6433–6437 (1992)
Stahl, S. J., Stewart, K. R. and Williams, F. D.: Extracellular slime associated with *Proteus* mirabilis during swarming. J. Bacteriol. **154**, 930–937 (1983)
Sturdza, S. A.: Expansion immédiate des *Proteus* sur milieux gélosés, Arch. Roum. Path. Exp. Microbiol., **32**(4), 543–562 (1973a)
Sturdza, S. A.: La réaction d'immobilisation des filaments des *Proteus* sur les milieux gélosés, Arch. Roum. Path. Exp. Microbiol., **32**(4), 575–580 (1973b)
Sturdza, S. A.: Développement des cultures de *Proteus* sur Gélose nutritive après mise en contact avec un milieu neuf, Arch. Roum. Path. Exp. Microbiol., **32**(2), 179–183 (1973c)
Williams, F. D. and Schwarzhoff, R. H.: Nature of the swarming phenomenon in *Proteus* Ann. Rev. Microbiol. **32**, 101–122 (1978)